

Seismic Analysis of URM Buildings in S. Africa

Trevor N. Haas, Thomas van der Kolf

Abstract—South Africa has some regions which are susceptible to moderate seismic activity. A peak ground acceleration of between 0.1g and 0.15g can be expected in the southern parts of the Western Cape. Unreinforced Masonry (URM) is commonly used as a construction material for 2 to 5 storey buildings in underprivileged areas in and around Cape Town. URM is typically regarded as the material most vulnerable to damage when subjected to earthquake excitation. In this study, a three-storey URM building was analysed by applying seven earthquake time-histories, which can be expected to occur in South Africa using a finite element approach. Experimental data was used to calibrate the in- and out-of-plane stiffness of the URM. The results indicated that tensile cracking of the in-plane piers was the dominant failure mode. It is concluded that URM buildings of this type are at risk of failure especially if sufficient ductility is not provided. The results also showed that connection failure must be investigated further.

Keywords—URM, Seismic Analysis, FEM.

I. INTRODUCTION

EARTHQUAKES are very common natural hazards, which, depending on its magnitude could lead to catastrophic disasters. Countries such as Haiti, New Zealand, Japan, for examples, have recently experienced catastrophic damage caused by earthquakes, resulting in billions of dollars of damage and significant loss of human life. Table I shows a list of earthquakes which caused the greatest number of fatalities since 2000 [1]. Based on this data it is evident that moderate intensity earthquakes, such as the Haiti earthquake, can result in catastrophic calamities with respect fatalities and its overall effect on the country's economy. We notice that in the case of Haiti, which experienced a moderate intensity earthquake, the estimated damage was more the double the country's annual GDP. A natural disaster of this magnitude obviously has a devastating effect on the country's economy.

The degree of damage the building can sustain is a function of many aspects but can mainly be attributed to the magnitude of the earthquake as well as the design and construction standards. Countries that do not have or have ineffective seismic provisions in their relevant building codes of practice are more at risk of sustaining major damage and even collapse of civil engineering infrastructure. Therefore, it is important for countries that are at risk of moderate to severe seismic activity require a robust seismic code of practice to ensure that its civil engineering infrastructure can resist the effects of earthquake loading.

T. N. Haas is with the Department of Civil Engineering, Stellenbosch University, Private bag X1, 7602, Matieland, Stellenbosch, South Africa (e-mail: trevor@sun.ac.za).

T. van der Kolf completed his Masters' degree thesis in December 2013. He is working as a structural design engineer at Uhambiso Consult in Port Elizabeth, South Africa (e-mail: tvanderkolf@uhambiso.co.za).

South Africa can be considered seismically stable based on the seismic hazard map [5]. This map indicates that the majority of the country could be exposed to a maximum peak ground acceleration (MPGA) of 0.05g with a 10% probability of being exceeded in 50 years. In addition the general public and government officials do not perceive earthquakes as a major threat due to its scarcity. This however raises a false sense of comfort as the same seismic map also shows certain regions in the Western Cape Province of South Africa to be susceptible to a MPGA of 0.15g. The same region is at risk to a much greater MPGA of 0.20g to 0.27g [6]. Therefore, this region is susceptible of experiencing moderate to strong PGA's, which has the ability to cause significant damage to civil engineering infrastructure which are poorly designed / not designed for seismic excitation.

TABLE I
MOST DESTRUCTIVE EARTHQUAKE IN TERMS OF FATALITIES SINCE 2000

Country	Richter Magnitude [2]	Fatalities [2]	Estimated damaged caused [3]	Estimated GDP at time of earthquake [4]
Haiti	7.0	316 000	\$ 14 Bil	\$ 6.5 Bil
Sumatra	9.1	227 898	\$ 4.5 Bil	\$ 256 Bil
China	7.9	87 587	\$ 150 Bil	\$ 4 522 Bil
Pakistan	7.6	80 361	\$ 5.2 Bil	\$ 110 Bil
Iran	7.4	50 000	\$ 7.2 Bil	\$ 116 Bil
Iran	6.6	31 000	\$ 1.9 Bil	\$ 135 Bil
Japan	9.0	20 896	\$ 309.0 Bil	\$ 5 897 Bil
India	7.7	20 023	\$ 5.5 Bil	\$ 494 Bil

Previous international research work shows that URM is a brittle material with low tensile strength and limited post cracking deformation capacity [7]. Masonry exhibits a non-homogeneous behaviour due to the distinct material properties of bricks and mortar as well as the complex material interactions. Experimental tests show that the properties of the masonry material are not a linear combination of the clay bricks and mortar's material properties [8]. Different mortar strengths and brick strengths as well as construction quality and material workability cause the masonry properties to vary significantly; [9]-[12]. Therefore, the uncertainties regarding masonry's material properties make the evaluation of the seismic performance of URM building extremely difficult. URM buildings require a sound conceptual design to account for the many uncertainties associated with URM and seismic loads [7]. Research also shows that URM structures performed poorly during past earthquakes of low to moderate seismicity and is also considered the most vulnerable construction material when subjected to seismicity, [7], [13]. URM structures are therefore not recommended for construction in

regions of moderate to severe seismicity due to their poor performance [14].

These apartments in the Western Cape Province of South Africa were designed and constructed prior to the first South African loading code of practice, SABS 0160 - 1989, which presented guidelines for determining seismic loading on civil engineering infrastructure. In 2009, South Africa adopted a new seismic loading code, SANS 10160 Part 4, which is in principle based on Eurocode 8 and almost a verbatim repetition thereof. SANS 10160 Part 4 is more comprehensive than its predecessor, SABS 0160. Since the implementation of the SANS 10160 Part 4, many questions have arisen whether these apartments are safe and meet the new code requirements. Due to the past political situation in South Africa, the seismically prone area of the Western Cape was demarcated for the construction of low income apartments, 2 to 5 stories high, in close proximity to one another. All apartments in this region were constructed of unreinforced masonry (URM) with varying plan dimensions. No credible probability of failure can be assigned to these URM apartments as no previous research work was conducted to determine its structural integrity. This puts the communities living in these apartments at risk if these buildings are subjected to a moderate intensity earthquake. Therefore the focus of this study was to determine whether these low income apartments can sustain a moderate intensity earthquake and whether the apartments meet the requirements of SANS 10160 Part 4 and the relevant masonry code of practice, SABS 0164.

II. METHOD

It is impractical and expensive to conduct experimental tests on a full scale or scaled models of a representative low income apartment. It was therefore decided to conduct the research using a finite element (FE) approach. This required that various properties, such as; the elastic's compressive and tensile stresses, the in- and out-of-plane Young's Moduli, the Poisson's ratio and the damping characteristics be determined for incorporation into the FE model. This section describes how these parameters were determined and how the FE model was calibrated to ensure reliable results. A brief explanation is also given how various earthquakes were selected.

A. Material Model

URM is a non-homogeneous and anisotropic material. It is therefore necessary to account for this anisotropy by assigning different material properties in different directions. There are many ways to account for the non-homogeneous material behaviour when analysing URM buildings. The material can either be analysed on a micro or a macro level; [15]-[17]. In the micro material model the bricks and mortar are treated as separate materials. This is achieved by assigning each material with its own characteristics together with suitable interaction properties. The disadvantage of this type of material model is that it is time consuming and computer intensive and therefore impractical for modelling an entire building. Macro material models on the other hand represent the masonry as a single

homogeneous material by combining the bricks, mortar and their interaction properties. The material properties for the macro model can be obtained from experimental work. This type of model is more suited for modelling large full scale URM structures. It was therefore decided to adopt a macro model for computational efficiency in the FE analysis.

B. Wall Stiffness

URM walls are the primary load resisting elements in these buildings. Lateral loads are transferred through the floor diaphragm to the in-plane shear walls. These shear walls provide lateral stiffness to a structure and transfer the forces to the foundation system. URM have two primary loading directions during seismic excitation that should be accounted for; i.e. in-plane and out-of-plane loading [7]. Thus, a wall will have different stiffnesses when loaded in the in-plane and the out-of-plane directions due to the difference in aspect ratio, interlocking capacity and arrangement of the masonry units and mortar. This means that URM will have much less stiffness and therefore provide less resistance in the out-of-plane direction compared with the in-plane direction.

C. Out of Plane Wall Stiffness

There are numerous examples of experimental tests on quasi static out-of-plane behaviour of one-way spanning URM; [18]-[21]. Most of these tests were performed on single walls in one-way bending with various techniques used to simulate different boundary support conditions. Recently, Griffith et al. performed out of plane displacement tests on standard clay brick URM walls with portions of the lateral walls included to simulate the effect of two-way bending. By including portions of the in-plane walls, the lateral support fixity was accounted for, while allowing for in- and out-of-plane wall connections to respond realistically. A model used by Griffith et al, has dimensions of 3 to 4 m between lateral walls similar to the representative low income apartment [22]. This therefore provides the motivation for the use of the experimental test results presented by Griffith et al. to calibrate the out of plane properties of the URM. Three URM walls which were experimentally tested by Griffith et al., was modelled in ABAQUS to obtain the out-of-plane wall stiffness. This was achieved by conducting a linear FE analysis using shell elements (S4R: 4-node doubly curved shell elements) with appropriate material properties. Griffith obtained an out-of-plane Young's Modulus of 3.54GPa. The Young's Modulus in the FE model was adjusted to 2.544GPa to obtain similar out of plane displacements. Table II shows the experimental and FE out-of-plane results for different vertical pressures, solid walls and walls with openings.

TABLE II
OUT OF PLANE DISPLACEMENT RESULTS

Wall	Vertical pressure on wall σ_v (MPa)	Lateral pressure on wall (kPa)	Experimental displacement at first crack (mm)	ABAQUS displacement using E of 3.544 GPa (mm)
Solid	0.10	4.0	4.0	3.8
12% Opening	0.10	4.8	5.0	5.25
12% Opening	0.05	3.0	3.0	3.26

The calibrated FE Young's Modulus magnitude is 28% less than the value obtained through masonry prism compression testing. This is expected and can be explained by the difference in aspect ratio between the tested masonry prisms and the out-of plane bending of the wall. This affects the interlocking and cracking behaviour of masonry. The Young's modulus obtained through compressive testing of masonry prisms do not provide a realistic representation of the Young's Modulus of a complete wall in the out-of-plane direction. While the response of the wall was essentially linear-elastic, minor cracks formed leading to a slight reduction in the wall stiffness, and hence Young's Modulus.

D. In Plane Wall Stiffness

Since the in and out-of-plane walls have different stiffnesses, it was necessary to determine the in plane stiffness. This was achieved using the out-of-plane wall stiffness obtained in section II together with a two storey URM building which was experimentally tested by Yi [23]. Fig. 1 shows the plan layout of the building indicating the various percentage opening of each wall.

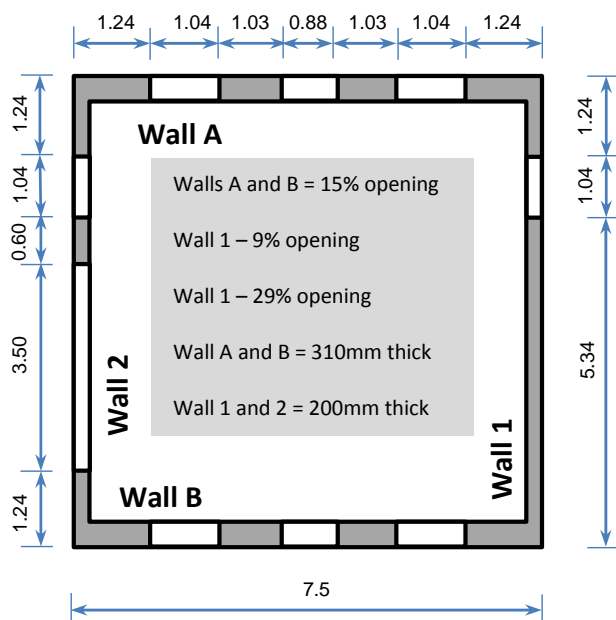


Fig. 1 Plan view of building used by Yi (2004)

This building was specifically chosen since the performance of the structure is well documented and is similar to the representative low income apartment which required investigation. Since the in-plane walls provide the majority of the lateral stiffness to the building, it follows

logically that lateral force displacement ($F - \Delta$) curves of a building can be used to determine in-plane wall stiffness. Using a full structure will also account for additional stiffness provided by out-of-plane walls due to coupling and flange effects. The floor diaphragm for the test structure is flexible and therefore only plays a minor role in redistributing lateral loads between in-plane walls. This greatly simplifies calibration of in-plane wall stiffness since the force displacement results will not be severely affected by the redistribution of forces through the diaphragm. Iteratively adjusting the Young's Modulus resulted in a value of $E = 5.7\text{GPa}$ for the in-plane wall stiffness. Table III presents the experimental and FE displacements together with the percentage differences.

TABLE III
IN-PLANE DISPLACEMENTS

Wall	Experimental Displacement (mm)	FE Displacement (mm)	Percentage Difference (%)
#1	0.86	0.90	4.8
#2	1.17	1.00	14.8

The displacement of Wall 1 was reproduced to within 5% of experimental values. Using the same Young's Modulus of 5.7 GPa, the displacement of Wall 2 was measured within 15% of the experimental value. Wall 2 has a very large opening ratio (29%) when compared to Wall 1 (9%). This leads to a less stiff wall as shown with the large experimental displacements. The FE model was not able to achieve the same lateral displacement for Wall 2. It is assumed that the larger displacements in the experimental results are as a result of the initiation of cracking due to smaller wall stiffness resulting in sensitivity to lateral force increase.

E. Finite Element Model

Two FE models were created in ABAQUS, using 4-node doubly curved S4R shell elements for the URM and floor diaphragms, while 2-node linear beam B31 elements were used for the lintels above opening, to model the behaviour of the building when excited from the East-West and the North-South directions. For each model, stiffnesses calibrated for the in- and out-of-plane behaviour presented in Section II, were applied to the in- and out-of-plane walls. A mesh sensitivity analysis was also conducted to ensure that appropriate accuracy was achieved. The material properties implemented in the FE model are summarized in Table IV.

TABLE IV
SUMMARY OF MATERIAL PROPERTIES IMPLEMENTED IN THE FINITE ELEMENT ANALYSIS

Material parameters	Magnitude
Compressive strength	$\sigma_y = 8.85\text{ MPa}$ $\sigma_{MAX} = 11.80\text{ MPa}$
Tensile strength (Max)	0.6 MPa
Poisson's ratio	0.2
Young's Modulus (E)	$E_{OUT\ OF\ PLANE} = 2.554\text{ GPa}$ $E_{IN\ PLANE} = 5.7\text{ GPa}$

The connections were assumed to be adequate in strength to resist seismic forces. The walls were modelled as pin connections at the base of the structure. Internal walls were connected with pin connections to floor slabs and fixed at their vertical edges to structural walls. The roof stiffness was neglected and it was added as a non-structural mass to the top of the structure. Floor slabs were tied to the structural walls using pin connections. A gap of 10mm was incorporated between the apex of the internal non-load bearing walls and the overhead slabs to prevent crushing of the internal masonry walls. The performance and capacity of the connections were not evaluated in this study since the connections and anchorage will depend on a specific building design and therefore vary from building to building.

F. Earthquake Selections

The previous general loading code of practice, SABS 0160, specified a MPGA of 0.15g with a 10% probability of being exceeded in 50 years for Cape Town and its surrounding areas. The new loading code dedicated to seismic loading specifies a MPGA of 0.10g with the same probability for the same area. Due to these inconsistencies with respect to the seismic intensity and the infrequency of earthquakes in this area, a number of moderate intensity earthquakes were selected to represent the possible range of earthquakes that could occur in Cape Town and its surrounding areas. The most unfavorable ground type was also selected. Six different earthquakes were chosen based on the above mentioned PGA, with a MPGA between 0.046g and 0.10. The Chalfant Valley earthquake was scaled to a PGA of 0.15g to account for the MPGA specified in the previous code, SABS 0160. The earthquake data is presented in Table V. This is the largest expected earthquake magnitude that could occur in the Western Cape with a probability of occurrence of 10% in 50 years as specified by the code. The acceleration response spectra of the earthquakes are presented in Fig. 2, together with the design response spectra of ground type D (soft soil) from SANS 10160-4. The response spectra apply a viscous damping ratio of 5%.

TABLE V
EARTHQUAKE DATA

	Magnitude (Richter)	PGA (g)
Chalfant Valley (1986) Station: CDMG 54424	5.77	0.095
Coalinga (1983) Station: CDMG 36452	6.36	0.091
Morgan Hill (1984) Station: CDMG 58117	6.19	0.046
Loma Prieta (1989) Station: CDMG 58117	6.93	0.100
Kobe (1995) Station: OSAJ	6.90	0.079
Chi-Chi (1999) Station: ILA 048	7.60	0.900

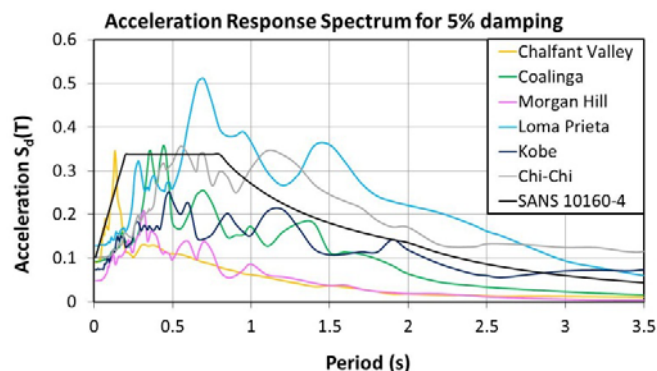
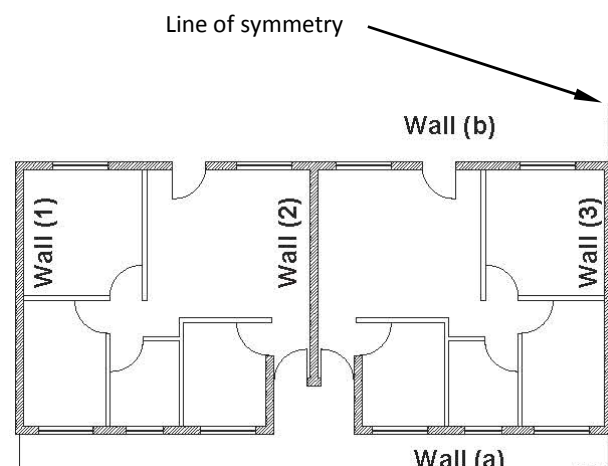


Fig. 2 Acceleration response spectra of selected earthquake with a 5% damping

From Fig. 2 the frequency content of the different earthquakes can be assessed. The Chalfant Valley earthquake responds primarily at lower periods. It is expected that this earthquake will cause increased excitations in short and stiff structures, such as typical three storey URM buildings. The Coalinga and Chi-Chi earthquakes match the design response spectrum in the constant branch of the curve. Both the Loma Prieta and Chi-Chi earthquakes show very large responses at larger natural periods. The Morgan Hill and Kobe earthquakes show smaller responses than the design spectrum. The diverse nature of the earthquake time histories allows a broad range of responses to be studied.



Shaded exterior walls are 270mm wide.
Shaded internal walls are 230mm wide.
All other internal walls are 110mm wide.

Fig. 3 Plan view of floor layout

III. ACTUAL BUILDING LAYOUT

The building chosen for this analysis is a three-storey URM low cost residential apartment building located in the Stellenbosch region of the Western Cape Province in South Africa. The structure has a simple layout and is considered a typical representation of a three storey apartment building constructed in low-income areas during the 1960's / 1970's.

The building has plan dimensions of 7.2 x 32m and consists of four apartment units per floor which are symmetrically arranged about the centre of the structure. Access to the units is provided via two external concrete staircases that are attached to the structure at floor levels. The staircases do not form part of the building's structural systems, and have their own supporting columns. The building was constructed using standard clay bricks with dimensions of 220 x 110 x 75mm with 10 mm mortar between the bricks. A plan layout of the structure is shown in Fig. 3, with structural walls indicated with a hatch pattern.

All external walls are cavity walls with two 110mm brick leaves and a 50mm cavity. Walls 2, 3 and 4 which separate the apartments are constructed as double leaf structural walls with a thickness of 230mm. The perimeter walls as well as the double leaf internal walls form the primary load bearing system with walls 1 to 5 acting as shear walls in the North-South direction and walls "a" and "b" acting as shear walls in the East-West direction.

Non-load bearing single brick width internal walls (110mm thick) is provided to partition the apartments. Although the partition walls do not carry vertical loads, they do however provide lateral support to the structural walls since they are built into the internal leaf of the structural walls to provide a moment fixed connection. Reinforced concrete slabs with a thickness of 250mm form the floor diaphragm system. The building has a simple, consistent and symmetrical layout in plan and along its height. Walls "a" and "b" have a large number of openings which accounts for doors and windows, while walls "1" and "5" have no openings in them. Shear walls are provided in both orthogonal directions allowing the building to resist forces due to seismic events both in directions. The perimeter shear walls should improve the resistance of the building to torsional effects.

IV. RESULTS AND DISCUSSIONS

A. Frequency Analysis

A natural frequency analysis was performed to determine the mode shapes and vibration frequencies of the structure. The significant modes were selected so that all modes with a

mass participation factor of 5% or more were included. In addition, the modes that contribute to 90% of the total participating mass were considered. The first 25 modes were selected based on the above mentioned criteria. Since the East-West and North-South models have different stiffness distributions (representing the reduced out-of-plane stiffness of URM), different natural frequencies were obtained as presented in Table VI. A comparison between the frequencies indicates the building responds primarily in the frequency range 8.8–13.4Hz. This indicates that the building will be affected to a greater extent by earthquakes with high excitation frequencies, i.e. low periods of vibration. The 0.15g Chalfant Valley earthquake in particular produces excitation in the high frequency range.

TABLE VI
SUMMARY OF THE THREE PRIMARY VIBRATIONS MODES ALONG WITH THEIR CORRESPONDING NATURAL FREQUENCIES FOR THREE DIFFERENT MODELS

Mode of Vibration	Modal Description	Frequency (Hz)		
		East – West Model	North - South Model	Uniform Stiffness Model
1	East – West Lateral Displacement	8.8	7.0	9.9
4	North – South Lateral Displacement	8.9	10.2	11.9
10	Torsional response	9.6	12.2	13.4

B. Modal Dynamic Linear Analysis

There are various numerical analyses methods available to analyse a structure under dynamic excitation. The modal dynamic analysis method is used to model material in its elastic state and therefore non-linear material behaviour cannot be implemented in this type of analysis. This method provides an efficient alternative to the complex non-linear analysis method such as the implicit dynamic analysis and was therefore chosen since it is ideal for evaluating the elastic response of a structure to many different time-histories. It is thus an ideal method for structures that respond primarily in the lower modes. The modal dynamic analysis will however not take the post cracking behaviour of masonry into account. As URM is a brittle material it is expected to have little post cracking capacity. The maximum elastic stresses obtained at key locations in the structure are presented in Tables VII and VIII for the East West and North South models.

TABLE VII
MAXIMUM ELASTIC STRESSES (MPA) AT KEY LOCATIONS IN THE EAST-WEST DIRECTION

	Chalfant (0.15g)	Chalfant Valley	Coalinga	Kobe	Loma Prieta	Morgan Hill	Chi-Chi
Tensile Stress In-plane Pier	1.00	0.63	0.29	0.28	0.36	0.21	0.29
Tensile Stress In-plane Non-Structural Wall	0.62	0.40	0.25	0.23	0.27	0.18	0.19
Compressive Stress In-plane Pier	0.99	0.63	0.29	0.27	0.35	0.21	0.28
Compressive Stress In-plane Non-Structural Wall	0.97	0.62	0.28	0.28	0.35	0.20	0.28
Tensile Stress at point of maximum shear	0.52	0.33	0.15	0.15	0.19	0.11	0.15
Sliding Shear Stress	0.55	0.35	0.21	0.20	0.23	0.15	0.16
Tensile Stress Connections Out-of-Plane Floor-to-Wall	0.29	0.18	0.11	0.10	0.12	0.08	0.09
Tensile Stress Connections In-Plane Floor-to-Wall	0.37	0.24	0.15	0.14	0.16	0.11	0.12
Tensile Stress Wall-to-Wall Connection	0.92	0.56	0.13	0.18	0.16	0.21	0.09
Compressive Stress Connections Out-of-Plane Floor-to-Wall	0.38	0.24	0.11	0.11	0.14	0.08	0.11
Compressive Stress Connections In-Plane Floor-to-Wall	0.50	0.31	0.15	0.14	0.18	0.10	0.15
Compressive Stress Wall-to-Wall Connection	0.95	0.60	0.12	0.18	0.17	0.20	0.11

TABLE VIII
MAXIMUM ELASTIC STRESSES (MPa) AT KEY LOCATIONS IN THE NORTH-SOUTH DIRECTION

	Chalfant (0.15g)	Chalfant Valley	Coalinga	Kobe	Loma Prieta	Morgan Hill	Chi-Chi
Tensile Stress In-plane Pier	0.66	0.42	0.21	0.21	0.26	0.10	0.20
Compressive Stress In-plane Pier	0.64	0.41	0.21	0.20	0.25	0.09	0.20
Tensile Stress at point of maximum shear	0.22	0.14	0.08	0.07	0.09	0.05	0.07
Sliding Shear Stress	0.28	0.15	0.08	0.07	0.09	0.05	0.07
Tensile Stress Connections Out-of-Plane Floor-to-Wall	0.30	0.19	0.09	0.09	0.12	0.04	0.09
Tensile Stress Connections In-Plane Floor-to-Wall	0.79	0.50	0.24	0.25	0.32	0.12	0.24
Tensile Stress Wall-to-Wall Connection	0.49	0.31	0.10	0.13	0.15	0.13	0.09
Compressive Stress Connections Out-of-Plane Floor-to-Wall	0.17	0.11	0.10	0.08	0.10	0.04	0.07
Compressive Stress Connections In-Plane Floor-to-Wall	0.75	0.48	0.26	0.23	0.30	0.11	0.23
Compressive Stress Wall-to-Wall Connection	0.48	0.31	0.10	0.15	0.15	0.13	0.09

Stresses obtained at key locations of the structure, which is shown in Tables VII and VIII were compared to the material yield strengths, shown in Table IV, to determine whether cracking, and possibly failure would occur. From Table VII we notice that the tensile stresses of the in-plane piers and the in-plane non-structural walls exceed the masonry's tensile strength of 0.6 MPa when subjected to the 0.15g Chalfant Valley earthquake. The tensile capacity of the in-plane piers were also exceeded when subjected to the 0.10g Chalfant Valley earthquake. None of the other low intensity earthquakes yielded tensile stresses greater than the codified allowable strength. This thus shows that if these structures are subjected to a moderate intensity earthquake it has a high probability of failure.

The structure showed no compression failure since the compressive stresses that developed were insignificant compared with the masonry's compressive cracking strength of 8.85MPa. The magnitudes of compressive stresses are comparable in size with the tensile stresses. The stresses which developed at the connections, however, significantly exceeded the codified limits for elements that do not form part of the main structural system. The probability of connection failure is therefore significant if the building was not designed to transfer large forces that developed at the connections.

The analysis also shows that there is a moderate probability that vertical cracks could form at the connection between the in and out-of-plane walls at the top storey of the structure. The stresses developed are, however, at the lower bound of SANS 10164-1 limits. This suggests that failure could occur if weak material is used. Diagonal shear stresses were within the limit for URM. Sliding shear is however likely to occur, especially after the formation of tensile cracks, since the shear stresses exceeded the unloaded shear resistance. Sliding shear will be especially critical if the building is unloaded since vertical compression loads are favorable to sliding shear resistance.

The results show that the building performs well for most of the earthquakes except for the Chalfant Valley earthquake. The 0.15g Chalfant Valley earthquake proved most critical. The building showed poor performance with a high probability of tensile and shear cracking as well as connection failure.

In the North-South direction, the maximum tensile strength was exceeded at the base of the in-plane shear walls for the 0.15g Chalfant Valley earthquake. The formation of cracks in

the shear walls will likely progressively reduce the strength of the shear wall during the rest of the excitation. Similar to the results of the East-West model, the connections experienced stresses which significantly exceeded the design strength specified in SANS 10164-1, suggesting high probability of failure. Unlike the case for the East-West direction, the North-South spanning shear walls performed well in both diagonal shear and sliding shear resistance. This can be attributed to the lack of openings in the North-South spanning shear walls.

The building performed better in the North-South direction than in the East-West direction. This is a result of the increased number of shear walls present in the North-South direction. The solid walls in the North - South direction increase the cross sectional area which provides additional shear resistance. Other factors such as the formation of stress concentrations at openings and the pier rocking mechanisms are also avoided. The building did however show that cracking at the heel/toe of the in-plane shear walls is likely to occur when subjected to the 0.15g Chalfant Valley earthquake. This is due in part to the reduced aspect ratio in the North-South direction leading to increased moments about the base of the structure. The effective performance of the building during small earthquakes of 0.10g is as a result of the good conceptual layout of the building as discussed in Section III. This further illustrates the importance of basic conceptual design guidelines especially when designing a building using a non-ductile material such as URM.

V. CONCLUSIONS

A representative three storey URM low income residential building located in the Western Cape Province was analysed to determine its response when subjected to low and moderate intensity earthquakes. The study revealed that:

- The building adhered to the conceptual layout requirements presented in SANS 10160-4 with its symmetric layout and good distribution of structural walls. Many lateral internal walls are provided at short distances apart which improves the response of the building to seismic events.
- The reason for the good structural layout is not necessarily a result of seismic code specifications. It is rather an indirect effect resulting from the simplicity of low cost residential buildings as these simple box

structures are easy to design and construct. These units are also very effective in carrying vertical loads due to the short internal spans of between 3 m to 5 m. The number of internal partition walls provides stability to the shear walls thereby enhancing its load bearing capacity. The small size of the apartments also means that long spans are avoided. Other unfavorable features such as soft storey's and discontinuities along the height of the structure are uncommon in residential URM structures located in underprivileged areas.

- The building has a large number of openings in the North and South facing perimeter walls. This could be problematic since these walls are the only structural walls that act as shear walls in the East–West direction. Also, stress concentrations normally form at the corners of openings leading to diagonal cracks. The presence of pier walls with small aspect ratios between window openings could lead to pier rocking failure that could result in the failure of one or more piers or the loss of equilibrium leading to collapse of the wall.
- These types of URM buildings are susceptible to earthquakes with high excitation frequencies, such as the 0.15g Chalfant Valley earthquake, which led to a disproportionate response compared with other earthquakes.
- For the excitation in the North–South direction, the extent of the cracking is unlikely to cause failure for the selected earthquakes due to the number and length of shear walls provided.
- The maximum tensile strength was exceeded in many piers in the East–West direction for the 0.15g Chalfant Valley earthquake. This suggests a high probability of a pier rocking mechanism developing. Although a pier rocking mechanism could be stable under cyclic loading, the mechanism has a large potential of becoming unstable, leading to failure. In addition to tensile cracking, sliding shear was identified as a likely failure mode for in-plane piers in the East–West direction.

It is concluded that a typical URM building has a high probability of failure during 0.15g magnitude earthquakes or to be damaged to an extent where the structure is unsafe for use.

ACKNOWLEDGMENT

The financial assistance of the Department of Civil Engineering at Stellenbosch University, Stellenbosch University's Department of Research Development and the National Research Foundation (NRF) towards this research is hereby acknowledged. Opinions expressed and conclusions arrived at, are those of the author and are not necessarily to be attributed to the NRF.

REFERENCES

[1] USGS, Earthquake Facts and Statistics, March 2014, <http://earthquake.usgs.gov/earthquakes/eqarchives/year/eqstats.php>, 28 May 2014.

[2] USGS, Largest and Deadliest Earthquakes by Year, October 2012, <http://earthquake.usgs.gov/earthquakes/eqarchives/year/byyear.php>, 28 May 2014.

[3] Bloomberg, Japan Sees Quake Damage Bill of up to \$309 Billion, Almost Four Katrinas, March 2011, <http://www.bloomberg.com/news/2011-03-23/japan-sees-quake-damage-bill-of-up-to-309-billion-almost-four-katrin.html>, 28 May 2014., Inter-American Development Bank, Haiti reconstruction cost may near \$14 billion, IDB study shows, February 2010, <http://www.iadb.org/en/news/webstories/2010-02-16/haiti-earthquake-reconstruction-could-hit-14-billion-idb,6528.html>, 28 May 2014, the guardian, Sichuan quake: China's earthquake reconstruction to cost \$150bn, August 2008, <http://www.theguardian.com/world/2008/aug/15/chinaearthquake.china>, 28 May 2014., Earthquake Page of Dr. George P.C., 2007, www.drgeorgepc.com/Earthquake2001India.html, 28 May 2014.

[4] The World Bank, Data, Countries and Economies, 2014, <http://search.worldbank.org/>, 28 May 2014.

[5] Wium, J. (2010), Background to draft SANS 10160 (2009): part 4 seismic loading, *Journal of the South African Institution of Civil Engineering*, Vol.52 No.1 April 2010, pp 20–27

[6] Kijko, A., Retief, S. J. P., and Graham, G. (2002). Seismic hazard and risk assessment for Tulbagh, South Africa: Part I—assessment of seismic hazard. *Natural Hazards*, 26(2):175–201.

[7] Tomaževič, M. (1999). Earthquake-resistant design of masonry buildings, Volume I of *Innovation in Structures and Construction*. Imperial College Press, London

[8] McNary, W. S. and Abrams, D. P. (1985). Mechanics of masonry in compression. *Journal of Structural Engineering*, 111(4):857–870.

[9] Lane, J. W., Watermeyer, R. B., and De Villiers, P. D. (1991). Masonry materials and design for movement. SAICE lecture course, Structural Division, Johannesburg, South Africa.

[10] Ewing, B. D. and Kowalsky, M. J. (2004). Compressive behavior of unconfined and confined clay brick masonry. *Journal of Structural Engineering*, 130(4):650–661.

[11] Ip, F. (1999). Compressive strength and modulus of elasticity of masonry prisms. *PhD thesis*, Carleton University.

[12] Bosiljkov, V. Z., Totoev, Y. Z., and Nichols, J. M. (2005). Shear modulus and stiffness of brickwork masonry: An experimental perspective. *Structural Engineering and Mechanics*, 20(1):21–44.

[13] Bruneau, M. (1994). State-of-the-art report on seismic performance of unreinforced masonry buildings. *Journal of Structural Engineering*, 120(1):230–251.

[14] Page, A. W. (1996). Unreinforced masonry structures—an Australian overview. *Bulletin-New Zealand national society for earthquake engineering*, 29:242–255.

[15] Truong Hong, L. and Laefer, D. F. (2008). Micro vs. macro models for predicting building damage due to underground movements, *The International Conference on Computational Solid Mechanics*, 2008.

[16] Bakhteri, J., Makhtar, A. M., and Sambasivam, S. (2004). Finite element modelling of structural clay brick masonry subjected to axial compression. *Jurnal Teknologi B*, 41(B):57–68.

[17] Lourenco, P. (1996). Computational strategies for masonry structures, *Ph.D. thesis*, Technische Universiteit Delft.

[18] Hendry, A. W. (1973). The lateral strength of unreinforced brickwork. *The Structural Engineer*, 51(2):43–50.

[19] Lawrence, S. J. (1983). Behaviour of brick masonry walls under lateral loading. PhD thesis, The University of New South Wales.

[20] Simsir, C. C., Aschheim, M. A., and Abrams, D. P. (2004). Out-of-plane dynamic response of unreinforced masonry bearing walls attached to flexible diaphragms. In *Proceedings of the 13th World Conference on Earthquake Engineering*, pages 1–4, Vancouver, BC.

[21] Ghobarah, A. and El Mandoh Galal, K. (2004). Out-of-plane strengthening of unreinforced masonry walls with openings, *Journal of Composites for Construction*, 8(4):298–305.

[22] Griffith, M. C., Vaculik, J., Lam, N. T.-K., Wilson, J., and Lumantarna, E. (2007). Cyclic testing of unreinforced masonry walls in two-way bending. *Earthquake Engineering & Structural Dynamics*, 36(6):801–821.

[23] Yi, T. (2004). Experimental investigation and numerical simulation of an unreinforced masonry structure with flexible diaphragms. *PhD thesis*, Georgia Institute of Technology.

Trevor Haas is a Senior Lecturer in Structural Engineering at Stellenbosch University. He obtained the National Diploma (1991) and National Higher Diploma (1992) in Civil Engineering from the former Peninsula Technikon, now Cape Peninsula University of Technology. In 1999 he was awarded the M.S. in Civil Engineering from Southern Illinois University at Carbondale, USA. In 2007 he was awarded a Ph.D. from Stellenbosch University. His research interests include numerical (FEA) modelling of steel structures, retrofitting of existing structures, structural dynamics and engineering education.

Tom Van Der Kolf is a practicing structural engineer at Uhambiso Consult, an engineering consulting company in Port Elizabeth. He completed a Bachelor of Engineering degree in Civil Engineering at Stellenbosch University in 2011 and continued to complete his Master's degree in Structural Engineering in 2014. His areas of interest include: design of concrete and steel structures, seismic design and structural dynamics.